Efficient Real-Time EV Charging Scheduling via Ordinal Optimization

Teng Long , *Student Member, IEEE*, Qing-Shan Jia , *Senior Member, IEEE*, Gongming Wang, *Member, IEEE*, and Yu Yang , *Member, IEEE*

Abstract—The surge of plug-in electric vehicles (PEV) on the roads poses the issue to handle the substantial charging demand. Particularly, the operation of charging stations requires an efficient and scalable real-time scheduling method to accommodate the dramatic charging requests in an economical (i.e., to best utilize the local renewable generation) and friendly (i.e., to reduce the impact on the electric grid) manner. This paper fulfills the objectives and makes the following main contributions. *First*, we develop a parameterized aggregated PEV charging model using the energy boundaries to express the charging flexibility. We propose to parameterize the aggregated charging policy by the incomplete Beta function based on the problem structures. The proposed model can scale down the decision variables from $O(NH)$ to $O(2)$ where N is the number of PEVs and H is the number of prediction horizon. *Second*, we develop an ordinal optimization (OO) based method (denoted as OO-P) to search for good enough charging policies within seconds while still providing probabilistic performance guarantee. *Third*, we demonstrate the performance of the proposed OO-P via simulations. The numerical results show that the solution of OO-P is only 4% worse than the optima. However, OO-P shows high computation efficiency and scalability. Compared with the existing real-time PEV charging scheduling method, OO-P can reduce 6% of the operation cost for the charging station. OO-P is also shown to outperform the existing heuristic rule.

Index Terms—Electric vehicle, ordinal optimization, stochastic programming.

NOMENCLATURE

t	Time index.
i	PEV index.
N	Charging station service capacity (The number of charging piles).
$\beta^g(t)$	Time-of-Use price (CNY/kW).
η^c	Efficiency of charging piles.
c^s	Amortized maintenance cost of charging station (CNY/kW).
c^r	Amortized maintenance cost of renewable energy system (CNY/kW).
E^{cap}	Battery capacity of PEV (kW h).
E	The aggregated energy charging profile (kW h).
E^+	Aggregated upper energy boundary curve (kW h).
E^-	Aggregated lower energy boundary curve (kW h).
e_i^+	Upper energy boundary curve of PEV i (kW h).
e_i^-	Lower energy boundary curve of PEV i (kW h).
$P^g(t)$	The purchased power from the grid (kW).
$P^w(t)$	Wind power (kW).
$P^{cap,\,w}$	The nominal power of wind turbine (kW).
$P^{PV}(t)$	Solar power (kW).
$P^{PV,\,w}(t)$	The nominal power of solar panels (kW).
$P^a(t)$	The total renewable generation power (kW).
$P(t)$	The total charging power of the parked PEVs (kW).
$P^{base}(t)$	The base load of the building (kW).
$P_i(t)$	The charging power of PEV i (kW).
$SoC_i(t)$	The State-of-Charge of PEV i.
SoC_i^d	The desired SoC of PEV i at leaving.
t_i^a/t_i^d	The arrival/departure time of PEV i.
$A^H(t)$	The stored hydrogen in the HES.
A^{cap}	The hydrogen energy storage capacity.

I. INTRODUCTION

THE PLUG-IN electric vehicle (PEV) is being surging on the roads at an annual pace of millions. It has been predicted that the global stock will reach nearly 140 millions, accounting for 7% of the global vehicle fleet and around 4% of global annual electricity demand by 2030 [1]. The induced charging demand has emerged as an urgent issue to be handled both for the power system operation and the transport electrification transition [2]. If not appropriately controlled, the substantial and spontaneous charging demand would cause grid congestion, inflate demand peaks and degrade power quality (e.g., voltage and frequency fluctuation), challenging the normal operation of power system [3]. On the other hand, if the PEVs can not be "fueled" as demanded, it will slow down the commercial rollout. To handle the PEV charging demand, we have seen the renewable-powered commercial charging

infrastructures are mounting everywhere [4]. As a major type of flexible load, the PEV charging demand deems to be largely filled by the green renewable supply, thus reducing the pressure on the grid [5]. Yet it relies on an efficient and scalable charging scheduling mechanism for the charging station (CS) to shape the partially controllable PEV charging demand to align with the non-dispatchable renewable supply.

Over the years, various solution methods have been studied for PEV charging scheduling. Some comprehensive review can be found in [6]–[8], where the methods can usually be distinguished by the way of addressing the computation burden caused by the scale and uncertainties of the problem. Particularly, as the charging sessions of PEVs usually extend their entire parking duration, the problem is a recursive multi-period optimization problem comprising a large number of decision variables and temporally binding constraints imposed by the heterogeneous charging requests. Moreover, the optimal PEV charging scheduling should enable the best utilization of local renewable for supplying the charging demand which are both dynamic and uncertain, further compounding the computational complexity.

To address the computational intensity, decentralized or distributed methods have drawn dramatic attention from the research communities (see [9]–[11]). These methods usually can achieve high computational efficiency and scalability by distributing the computation to individual PEVs via a certain price mechanism. Moreover, the vehicle-centric implementations are usually suitable for accounting for individual charging preferences. However, when we face a systematic objective such as the total operation cost for the CS that requires the full cooperation of multiple PEVs, it may not work well due to two underlying issues. *First*, the decentralized methods usually rely on the assumption that the individuals are sensitive to the uniform charging price. *Second*, the convergence of decentralized methods depend on a well-designed price mechanism which is actually subtle especially with the presence of non-smooth and non-convex objective or constraints (decentralized optimization for non-smooth and non-convex problems is still an unresolved direction [12]). Some other way to handle the computation burden for real-time practice is to employ heuristic methods or rules, such as [13]–[15]. The main idea is to develop some static and descriptive charging rules based on our sense and understanding of the problems. These methods are usually easy to implement but subject to the drawback of no systematic performance guarantees and big room for performance improvement.

Another way to handle the computation complexity is to find *non-anticipative* robust solution from off-line learning, i.e., the on-line implementation will make decisions only regard to the current system state. Stochastic optimization [16], scenario-based stochastic programming [17]–[19] or dynamic programming [20]–[22] have been extensively studied for that category. However, they mostly suffer computational challenges from the well-known curse of dimensionality (i.e., large state and action space, a large number of scenarios to capture the features of uncertainties). It was reported that it will take hours to solve the stochastic programming problem for the PEV charging scheduling even for a moderate scale [17].

Deep reinforcement learning methods (DRLs) have received widespread interest by proposing to use neural networks or feature functions to alleviate the computation burden for the problem [23]–[26]. However, note that the performance of DRLs depends on the neural network design and feature function recognition, which is challenging and subtle. Moreover, the implementation of these methods require substantial and historical data to capture the patterns and uncertainties of the renewable generation and the dynamic PEV charging demand.

Overall, we have seen substantial endeavor for handling the computation burden of PEV charging. As discussed above, some works have aimed for robust solutions from off-line learning, such as the programming and learning based methods, whereas some have proposed to design decentralized implementation or developing heuristic rules. Yet these methods still face obstacles for the CS operation in practice. *First*, the group of served PEV customers are dynamically changing over the time and the historical driving pattern data required by learning-based method are usually not available to the CS. Moreover, the well-tuned model offline may not adapt to the expansion of the PEV market. *Second*, though decentralized methods favor computational efficiency but it is hard to uniformly price the service for the CS to achieve the profit-maximization objective.

Motivated by the practice, we studies the real-time PEV charging scheduling in the shoes of the CS in this paper. We aim for an efficient and scalable method to minimize the operation cost of the CS with performance guarantee under uncertainties. To fulfill the objective, we make the following contributions.

(C1) We develop a parameterized aggregated PEV charging model using the energy boundaries to express the charging flexibility. We parameterize the aggregated charging profile in array by the incomplete Beta function by exploring the problem structures. This model can scale down the decision variables from $O(NH)$ to $O(2)$ where N is the number of PEVs and H is the number of prediction horizon.

(C2) We develop an ordinal optimization (OO) based method (denoted as OO-P) to search for the good enough solutions for the aggregated problem within seconds while still providing probabilistic performance guarantee. Further, we propose an modified Less Laxity and Longer Remaining Processing Time (MLLLP) principle based method to distribute the aggregated charging profile across the parked PEVs. The proposed MLLLP method can provide a full charging order while still preserving the performance of the existing LLLP principle [27]. We prove that the MLLLP principle based method guarantees to find a feasible solution whenever it exists under mild assumptions (Theorem 1).

(C3) We demonstrate the performance (i.e., reducing operation cost and computational efficiency) of the proposed OO-P via simulations. The results show that the performance degradation is no more than 4% compared with the optimal solution obtained from solving
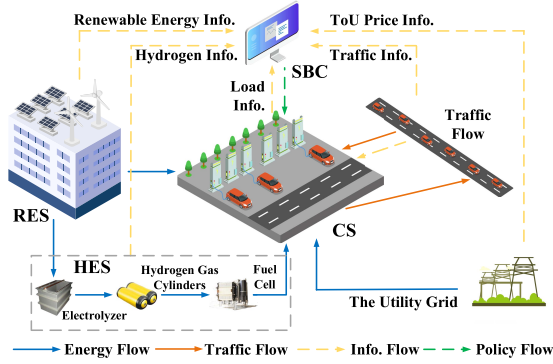
Fig. 1.   A charging station operated by a smart building.

a large-scale multi-period optimization problem comprehensively. However, OO-P can solve the problem within seconds. Comparing with the existing real-time PEV charging method, OO-P can further reduce the CS operation cost by 6%. Beside, OO-P is also shown to outperform the existing heuristic rule in optimizing the CS operation cost for the CS.

The rest of the paper is organized as follows. We introduce the problem definition and formulation in Section II, introduce the OO-based method in Section III, present numerical results in Section IV, and finally conclude in Section V.

II. PROBLEM FORMULATION

A. Charging Station Configuration

We consider a public CS run by a smart building as in Fig. 1. The building is fitted with a renewable energy system (RES) comprising wind turbines, solar panels and a hydrogen energy storage (HES). Like other energy storage techniques, the HES can be "charged and discharged" to enhance the balance between generation and consumption. Besides, the HES has some distinctive features such as high storage capacity and enabling the conversion of different energy types, being popular with energy system today.

In our setting, the renewable generation can be used to support the building's base load (non-elastic) or delivered to the CS for charging service. When it is not enough, the building can purchase the shortfall from the grid by paying the Time-of-Use (ToU) price. Conversely, if there is excess renewable energy, it can be converted to hydrogen and stored in the HES, and re-electrified at the required time period (discharging) [28].

In practice, the PEVs will arrive at the CS with certain charging requirements. When an PEV arrives, it will propose the charging request (i.e., parking duration and the charging demand) to the CS. Then, the CS is expected to respond quickly by deciding its admission and returning the charging plan (when the charging capacity has been fully occupied, the CS will have to give up the new arrivals, however we assumes sufficient service capacity in this paper).

Since both the building itself and the CS consume energy, the whole system is coordinated by a smart building controller (SBC) for minimizing the total operation cost. We assume

the building load is non-elastic and the CS will negotiate the charging fees with individual PEV customers endogenously, therefore the problem of maximizing the CS profit reduces to minimize its total operation cost.

Before giving the problem formulation, we clarify our main assumptions as below.

(A1) The PEV users will report their charging requests (i.e., parking duration and charging demand) to the CS at arrival.

(A2) The CS has sufficient service capacity for the PEV charging requests and we don't consider admission control.

(A3) The HES is only used to store the surplus renewable generation not the electricity purchased from the grid.

B. Real-Time Scheduling Model

We consider the operation of an CS over the discretized optimization horizon $t \in \mathcal{T} \triangleq \{1, 2, \ldots, T\}$ where t denotes the computing epoch and ΔT denotes the decision interval. The CS has installed N charging piles (i.e., service capacity) and the PEVs are labeled by $\mathcal{N} \triangleq \{1, 2, \ldots, N\}$ in our formulation. We consider the real-time scheduling in the sense that at each time t_0 the charging decision is made based on i) the charging requests of the parked PEVs $\mathcal{I}(t_0)$, and ii) the predictions of renewable generation over the predicted horizon H. In the following, we introduce the dynamics of the PEVs, RES and HES, respectively.

1) PEV: At each time $t \in [t_0, t_0 + H)$, we represent the charging request of the parked PEV by 4 tuples $(t_i^a, t_i^d, SoC_i(t), SoC_i^d)$, $\forall i \in \mathcal{I}(t_0)$ which includes the arrival and departure time t_i^a and t_i^d, the current state-of-charge (SoC) $SoC_i(t) \in [0, 1]$, and the desired $SoC_i^d \in [0, 1]$ at leaving.

Amid the charging process, the charging power of each parked PEV i is restricted by the nominal charging power of charging piles P^{rated} and the PEV's remaining charging demand to fill $(SoC_i^d - SoC_i(t))E^{\text{cap}}$, i.e.,

$$0 \leq P_i(t) \leq \min\left\{P^{\text{rated}}, \left(SoC_i^d - SoC_i(t)\right)E^{\text{cap}}/\left(\eta^c \Delta T\right)\right\} \quad (1)$$

where E^{cap} denotes the battery capacity of PEVs and η^c denotes the charging efficiency.

Accordingly, the SoC dynamics can be modeled as

$$SoC_i(t + 1) = SoC_i(t) + P_i(t)\eta^c \Delta T/E^{\text{cap}} \quad (2)$$

To ensure the PEV charging requests to be fulfilled before the deadline, we impose the following feasibility constraint

$$\left(SoC_i^d - SoC_i(t)\right)E^{\text{cap}} \leq \left(t_i^d - t\right)P^{\text{rated}}\eta^c \Delta T. \quad (3)$$

2) RES: The RES supply encompasses the wind and solar generation. The wind power is determined by the instantaneous wind speed $v(t)$, the wind turbine configurations and number (i.e., cut-in speed v^{cutin}, cut-out speed v^{cutout}, rated speed v^{rated}, nominal power $P^{\text{cap,w}}$ and the number of turbines N^w). According to [29], the wind power can be estimated by

$$P^w(t) = \begin{cases} N^w P^{\text{cap,w}}, & v^{\text{rated}} \leq v_t \leq v^{\text{cutout}} \\ N^w P^{\text{cap,w}}\left(\dfrac{v(t)}{v^{\text{rated}}}\right)^3, & v^{\text{cutin}} \leq v_t \leq v^{\text{rated}} \\ 0, & \text{otherwise} \end{cases} \quad (4)$$

The solar power is determined by the instantaneous solar radiation intensity $G^{PV}(t)$ and solar panel configurations (i.e., nominal radiation intensity $G^{ref,PV}$, the nominal power $P^{cap,PV}$, and the efficiency of solar panel inverters f^{PV}) [30], which is

$$P^{PV}(t) = P^{cap,PV} f^{PV}\left(G^{PV}(t)/G^{ref,PV}\right) \quad (5)$$

Thus, the total renewable supply at time t is

$$P^{a}(t) = P^{w}(t) + P^{PV}(t). \quad (6)$$

3) HES: In this paper, we do not consider the SBC feeding renewable into the grid. In other word, when there exists the RES supply over the total demand (i.e., the building base load plus the CS charging load), the surplus will be converted to hydrogen and stored in the HES for future use (charging). On the contrary, the stored hydrogen can be converted to the electric power to make up the gap between the supply and demand (discharging). At each time $t \in [t_0, t_0+H)$, the surplus or deficient renewable supply over the total demand is

$$P^{s+}(t) = \left[P^{a}(t) - P(t) - P^{base}(t)\right]_{+}$$
$$P^{s-}(t) = \left[P^{base}(t) + P(t) - P^{a}(t)\right]_{+} \quad (7)$$

where we define the operator $[x]_{+} \triangleq \max\{0, x\}$ for $x \in \mathbb{R}$. We have $P(t) = \sum_{i \in \mathcal{I}(t_0)} P_i(t)$, $\forall t \in [t_0, t_0 + H)$ which denotes the aggregated charging power of the parked PEVs.

The HES uses hydrogen as medium for energy storing and releasing. While storing the surplus renewable supply $P^{s+}(t)$, the produced hydrogen through electrolysis is [31]

$$n^{H}(t) = \eta^{F} I^{ae}(t) N^{ae}/2F = \eta^{F} P^{s+}(t) N^{ae}/2U^{ae}F \quad (8)$$

where $n^{H}(t)$ denotes the generated hydrogen in moles. η^{F} is the production efficiency and N^{ae} is the number of electrolyzers. $I^{ae}(t)$ and U^{ae} are the current and voltage of electrolyzers. F denotes the Faraday constant. After that, high-pressure gas cylinders are used for hydrogen storing. According to the Ideal Gas Law, we have

$$Q^{H}(t) = n^{H}(t)RT^{H}/p^{H} \quad (9)$$

where $Q^{H}(t)$ represents the hydrogen in volume. R is the universal gas constant. T^{H} and p^{H} denote the standard temperature and pressure of gas cylinders.

While the amount of energy is to be released, the stored hydrogen is converted to electrical power via fuel cell (discharging), and the discharged hydrogen power is [31]

$$P^{e}(t) = I^{H}(t)U^{H} = 2Q^{H}(t)FU^{H} \quad (10)$$

where $I^{H}(t)$ and U^{H} are the current and standard voltage of fuel cell.

Form (8)-(10), we can induce the round-trip efficiency for the HES as follows

$$\eta^{P2H} = \frac{N^{F}N^{ae}RT^{H}}{2U^{ae}FP^{H}} \text{ and } \eta^{H2P} = 2FU^{H}$$

Thus, we can model the dynamics of HES akin to other energy storage techniques as

$$A^{H}(t+1) = \begin{cases} \min\{A^{H}(t) + P^{s+}(t)\eta^{P2H}, A^{cap}\}, & P^{s+}(t) \geq 0 \\ \max\{0, A^{H}(t) - P^{s-}(t)/\eta^{H2P}\}, & P^{s-}(t) \geq 0 \end{cases}$$
$$(11)$$

When the stored hydrogen power is depleted and still not enough to satisfy the demand, the SBC is required to purchase the shortfall from the grid, which is denoted as

$$P^{g}(t) = \left[P(t) + P^{base}(t) - P^{H}(t) - P^{a}(t)\right]_{+} \quad (12)$$

where we have $P^{H}(t) = A^{H}(t)\eta^{H2P}$.

4) Optimization Problem: At each time t_0, we minimize the total operation cost for the CS over the predicted horizon $[t_0, t_0 + H)$ which comprises the electricity bill paid to the grid $P^{g}(t)\beta^{g}(t)$, the maintenance cost of the CS (i.e., charging piles) $c^{s}P(t)$ and the maintenance cost of the RES (i.e., wind turbines, solar panels and the HES) $c^{r}P^{a}(t)$, and we have the overall optimization problem as follows

$$J(t_0) = \min_{P_i(t)} \sum_{t=t_0}^{t_0+H-1} \left[P^{g}(t)\beta^{g}(t) + c^{s}P(t) + c^{r}P^{a}(t)\right]$$
$$s.t. \ (1) - (7), \ (11) - (12), \ \forall t \in [t_0, t_0 + H),$$
$$i \in \mathcal{I}(t). \quad (13)$$

Particularly, as the PEVs come and leave over the time and new arrivals may occur during $[t_0, t_0 + H)$, we only execute the charging decision for the current time t_0. For the next moment, we will compute the charging decision by repeating this process with the new arrivals involved.

We have built the PEV charging scheduling model in a real-time manner. Yet solving problem (13) directly is not desirable and scalable considering the computation burden. We are facing $O(HN)$ decision variables at each computing epoch which can be quite large and result in time-consuming solving process [17], [32]. The computation issue remains to be addressed.

III. SOLUTION METHODOLOGY

In this section, we establish a computationally efficient approach for handling problems (13) via soft optimization. The main idea includes three phases: *i)* scaling down the decision variables by aggregation, *ii)* searching good enough solutions via order optimization, and *iii)* deciding the charging decisions for individual PEV by a modified Less Laxity and Longer Remaining Processing Time (MLLLP) principle.

A. Aggregated PEV Charging Model

There usually exists flexibility regarding the individual PEV charging process. As we could imagine, the *fastest* way to accomplish the charging request is "plug and play," i.e., start uninterrupted charging at maximum rate at arrival until the desired SoC is achieved. Oppositely, the *slowest* way is to "standby and delay," i.e., delay the charging to the last moment. In light of that, the charging flexibility of a specific PEV i can be characterized by the energy boundaries (e_i^{+}, e_i^{-})
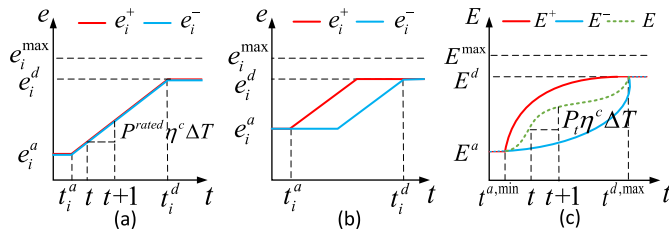
Fig. 2. The energy boundary curve. (a) uncontrollable charging process. (b) controllable charging process. (c) aggregated energy boundaries.

that represent the *fastest* and *slowest* charging process, respectively. The idea of using energy boundaries to capture PEV charging flexibility was first proposed in [33] and the energy boundaries (e_i^+, e_i^-) can be constructed by

$$e_i^-(t) = \max\left\{e_i^-(t-1), e_i^d - P^{\text{rated}}\eta^c\Delta T\left(t_i^d - t\right)\right\}, \quad (14\text{a})$$

$$e_i^+(t) = \min\left\{e_i^+(t-1) + P^{\text{rated}}\eta^c\Delta T, e_i^{\max}\right\},$$
$$\forall t \in [t_0, t_0 + H). \quad (14\text{b})$$

where $e_i^{\max} = E^{\text{cap}}$ denotes the battery capacity. Obviously, we have $e_i^+ \geq e_i^-$.

Empirically, the space between the upper and lower energy boundaries characterizes the PEV charging flexibility and any monotonically non-decreasing curve in-between represent a possible charging solution for the PEV. Therefore, it would be easy to visually identify the PEV charging flexibility from the energy boundaries (e_i^+, e_i^-) and we can differentiate them by *uncontrollable* and *controllable* charging process as in Fig. 2, where $e_i^a = SoC_i^a E^{\text{cap}}$, and $e_i^d = SoC_i^d E^{\text{cap}}$ denote the stored energy at arrival and the desired stored energy at leaving.

With the identified energy boundary model for individual PEV, it's reasonable to aggregate them as the aggregated energy charging profile which exclusively determines the total operation cost for the CS. Intuitively, the aggregated energy boundary model (E^+, E^-) for all parked PEVs is

$$E^{+/-}(t) = \sum_{i\in\mathcal{I}(t_0)} e_i^{+/-}(t), \quad t^{a,\min} \leq t \leq t^{d,\max} \quad (15)$$

where $t^{a,\min} = \min_{i\in\mathcal{I}(t_0)} t_i^a$ and $t^{d,\max} = \max_{i\in\mathcal{I}(t_0)} t_i^d$ are the earliest arrival and latest departure time for all parked PEVs.

We illustrate the aggregated energy boundary model in Fig. 2(c). Thus, any monotonically non-decreasing curve E in-between represents a possible solution for problem (13), and the aggregated charging power profile can be induced as

$$P(t) = (E(t+1) - E(t))/\left(\Delta T\eta^c\right), \forall t \in [t_0, t_0 + H). \quad (16)$$

Note that the aggregated charging profile $\boldsymbol{P} = [P(t)], \forall t$ determines the total operation cost defined in problem (13). Therefore, we can obtain an equivalent optimization problem for the CS by embodying the aggregated energy boundary

model as

$$J(t_0) = \min_{P(t)} \sum_{t=t_0}^{t_0+H-1} \left[P^g(t)\beta^g(t) + c^s P(t) + c^r P^a(t)\right]$$

$$s.t. \quad (4)-(7), \ (11)-(12),$$
$$E(t+1) = E(t) + P(t)\eta^c\Delta T,$$
$$E^-(t) \leq E(t) \leq E^+(t), \ \forall t \in [t_0, t_0 + H). \quad (17)$$

B. Soft Optimization Based on OO

To be noted, we have scaled down the decision variables from $O(HN)$ to $O(H)$ in problem (17). However, solving problem (17) is still time-consuming due to the bunch of temporally binding constraints. Therefore, we apply the ordinal optimization (OO) [34] to search for good enough solutions to achieve high computation efficiency.

The basic idea of OO is hardly new to us: *i)* Order is easier to identify than value, especially when there is noise or prediction error, and *ii)* the optima is usually very costly but not the good enough. Until the recent decades, OO has been developed as a systematic soft optimization technique with performance to be quantified [34], and found its various successful applications in power systems [35], file system [36] and manufacturing system [37], etc. OO is suitable for the performance improvement of complex systems by seeking good enough solutions via simulations instead of solving a complex optimization problem directly. In general, the significance of OO is to allow a trade-off between the computation burden and the performance based on the "No-free-Lunch" theory.

When it comes to problem (17), the problem can be translated into the search of energy charging profile $\boldsymbol{E}$ within the energy boundaries $(\boldsymbol{E}^-, \boldsymbol{E}^+)$. However, the decision variable $\boldsymbol{E} \in \mathbb{R}^H$ is in array and it is impossible to simulate the H-dimensional decision space. To handle this issue, we parameterize the policy $\boldsymbol{E}$ by exploring the problem structure: the energy charging profile $\boldsymbol{E}$ is monotonically non-decreasing. This feature suggests us to use the incomplete Beta function (characterized by two parameters α, β) to parameterize $\boldsymbol{E}$.

The incomplete beta function is characterized by two positive parameters $\alpha, \beta > 0$, and we have

$$F(y|\alpha, \beta) = \int_0^y f(z|\alpha, \beta)dz \quad (18)$$

where $f(z|\alpha, \beta) = Cz^{\alpha-1}(1-z)^{\beta-1}$ represents the probability density function with $C = \frac{\Gamma(\alpha+\beta)}{\Gamma(\alpha)\Gamma(\beta)}$ ($\Gamma(\cdot)$ represents the gamma function).

For any monotonically non-decreasing curve restricted to the unit square $[0, 1] \times [0, 1]$, it can be determined by the inverse function of $F(y|\alpha, \beta)$ as

$$\Delta(x|\alpha, \beta) = F^{-1}(x|\alpha, \beta) = F(x|1/\alpha, 1/\beta), \quad (19)$$

where $F(\cdot|\cdot, \cdot)$ can be evaluated via numerical approximation formulas. In this way, we can use two parameters α and β to represent any standard monotone nondecreasing curves [38].

We can normalize the aggregated energy boundary curve by dividing the vertical axis by $(E^d - E^a)$ and the horizontal axis
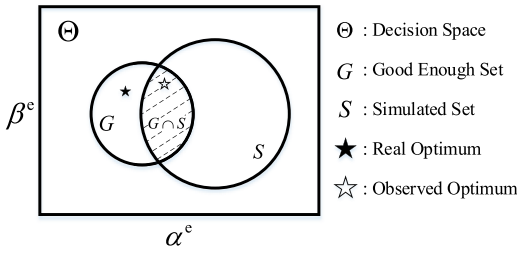
Fig. 3. Graphical illustration of OO for problem (21).

by $t^{\mathrm{d,max}} - t^{\mathrm{a,min}}$. Therefore, the policy E can be formulated by parameter α^{e} and β^{e} as

$$E(t) = \Delta\left(t / \left(\left(t^{\mathrm{d,max}} - t^{\mathrm{a,min}}\right) | \alpha^{\mathrm{e}}, \beta^{\mathrm{e}}\right)\right)\left(E^{\mathrm{d}} - E^{\mathrm{a}}\right) \quad (20)$$

By using the incomplete Beta function to parameterize the energy charging profile E, we can relax problem (17) to problem (21) with two decision variables α^e and β^e. This implies that we now have 2D decision space to be simulated and evaluated for OO implementation.

$$J(t_0) = \min_{\alpha^e, \beta^e} \sum_{t=t_0}^{t_0+H-1} \left[P^{\mathrm{g}}(t)\beta^{\mathrm{g}}(t) + c^{\mathrm{s}}P(t) + c^{\mathrm{r}}P^{\mathrm{a}}(t)\right]$$
$$s.t. \ (4)-(7), \ (11)-(12), \ (20),$$
$$E(t+1) = E(t) + P(t)\eta^c \Delta T,$$
$$E^-(t) \le E(t) \le E^+(t), \ \forall t \in [t_0, t_0+H). \quad (21)$$

Subsequently, we introduce the implementation of OO to search for good enough policies for problem (21). Fig. 3 shows the graphical illustration, where Θ denotes the feasible decision space for the parameters α^e and β^e. Particularly, the ranges can be determined by fitting the upper and lower energy boundaries (E^-, E^+) using incomplete Beta function. This implies that all the parameterized policies are feasible. G represents the **real** top-$|G|$ solutions among the whole decision space, which is usually known *a priori*. S represents the **simulated** decision space.

Based on the theory of OO [34], for a specified **Alignment Level** k, i.e., the **simulated** set S contains at least k solutions belonging to **real** good enough set G with the **Alignment probability** AP $= \mathrm{Prob}(|G \cap S| \ge k)$, the required size of S can be determined by the following formula

$$Z(k, g) = e^{Z_1} k^{Z_2} g^{Z_3} + Z_4 \quad (22)$$

where $g = |G|$ denotes the carnality of set G. The coefficients Z_1, Z_2, Z_3, Z_4 are determined by problem structure characterized by the 4 tuple (**OPC**, δ, **AP**, **SR**) (pp. 42, [39]). **OPC** denotes the class of the ordered performance curve (OPC) which is a plot of the objective value with respect to the ordered policies (i.e., the worst to the best). Conceptually, the **OPC** classes include "Flat," "U-Shaped," "Neutral," "Bell" and "Steep." δ represents the prediction error level of the renewable generation. **SR** is the selection rule including the options of "blind pick" and "horse race."

C. MLLLP

Once the aggregated charging policy E (or P) is decided by OO, the remaining problem is to distribute the charging power among the parked PEVs $\mathcal{I}(t_0)$. Related to this issue, [27] proposed the Less Laxity and Longer Remaining Processing Time (LLLP) principle. The significance of LLLP is to spot the dominated charging priority (order) among the parked PEVs from their charging laxity defined as

$$\theta_i(t) = \lambda_i(t) - \gamma_i(t) \quad (23)$$

where $\lambda_i(t) = t_i^{\mathrm{d}} - t$ denotes the remaining parking time of PEV i. $\gamma_i(t) = ((SoC_i^{\mathrm{d}} - SoC_i(t))E^{\mathrm{cap}}) / (P^{\mathrm{rated}}\eta^c \Delta T)$ represents the minimal charging period required to fulfill the remaining charging demand.

Based on the pairs $(\theta_i(t), \lambda_i(t))$, LLLP can provide a partial charging order described as below.

Definition 1 (LLLP: partial order) [27]: For any two PEV $i, j \in \mathcal{I}(t_0)$, we say $i \preceq j$ (j has higher priority in charging order over PEV i), if j has less laxity and longer remaining processing time, i.e., $\theta_i(t) \ge \theta_j(t)$, $\gamma_i(t) \le \gamma_j(t)$, and at least one of these two inequalities strictly holds.

LLLP can reduce the problem complexity without losing the optimality. However, there are two underlying issues for our application. *First*, it deals with the constant charging rate and we study the general case with varying charging rate (i.e., $[0, P^{\mathrm{rated}}]$). *Second*, it can only provide a partial charging order, i.e., we may encounter PEV i, j incomparable under LLLP (for example, $\theta_i(t) \ge \theta_j(t)$ and $\gamma_i(t) \ge \gamma_j(t)$ or the opposite). To handle the first issue, we always distribute the maximum charging rates to the PEVs with a higher charging priority. For the second issue, we propose a modified LLLP (MLLLP) principle based method to provide a full charging order.

Definition 2 (MLLLP: full order): For any two PEV $i, j \in \mathcal{I}(t_0)$, we say $i \preceq j$ (j has higher priority in charging order over PEV i) if we have: i) $\theta_i(t) > \theta_j(t)$ or ii) $\theta_i(t) = \theta_j(t)$ and $\gamma_i(t) \le \gamma_j(t)$.

The interpretation of MLLLP is to decide the charging order by taking two steps. *First*, decide the charging order of the parked PEVs by their laxity $\theta_i(t)$ in a non-decreasing order. *Second*, regulate the charging order within each group of parked PEV with *equal* laxity (e.g., $\theta_i(t) = \theta_j(t)$) with LLLP. The significance of MLLLP is to provide a full charging order while preserving the performance of LLLP. Besides, it can ensure the feasibility (i.e., the charging request of all parked PEV to be filled before leaving) under some conditions.

Theorem 1: For a monotonically non-decreasing energy charging profile E satisfying

$$E^-(t) \le E(t) \le E^+(t), \quad (24a)$$
$$E(t+1) - E(t) \ge \sum_{i \in \mathcal{J}(t_0)} \min\Big\{P^{\mathrm{rated}}\eta^c \Delta T,$$
$$\left(SoC_i^{\mathrm{d}} - SoC_{i,t}\right)E^{\mathrm{cap}}\Big\},$$
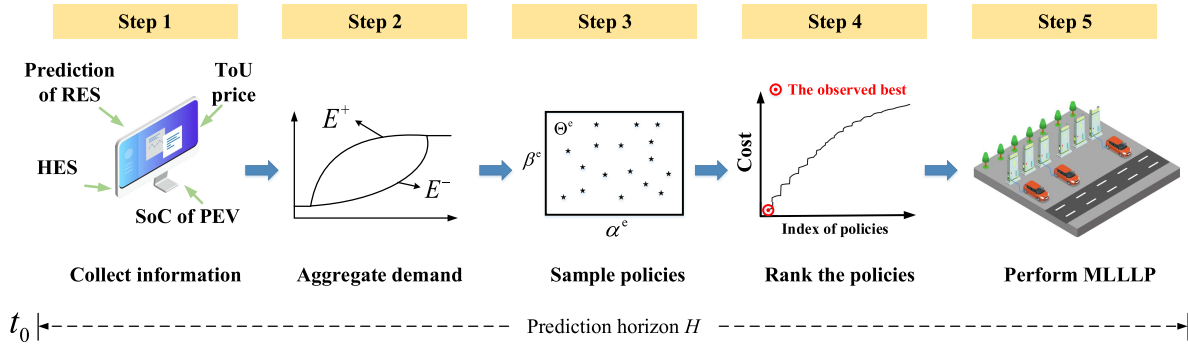$$\forall t \in [t_0, t_0+H), \quad (24b)$$

Fig. 4. The PEV charging scheduling based on ordinal optimization (OO).

TABLE I
PARAMETER SETTINGS

Wind & Solar		HES		PEV & CS	
Param.	Val.	Param.	Val.	Param.	Val.
$P^{cap,w}$	2400 kW	η^F	0.98	E^{cap}	75 kW h
v^{cutin}	2.5 m s^{-1}	U^{ae}	60V	P^{rated}	44 kW
v^{cutout}	22 m s^{-1}	R	8.314	η^c	0.92
v^{rated}	12 m s^{-1}	p^H	15 MPa	c^s	0.018 CNY/kW
N^w	2	U_k^H	400V V	c^r	0.018 CNY/kW
$P^{cap,PV}$	1500 kW	N^{ae}	8	P^{base}	200 kW
f^{PV}	0.88	F	96485.34		
$G^{ref,PV}$	800W W	T^H	300 K		

we can obtain a feasible charging policy for problem (21) based on MLLLP. $\mathcal{J}(t_0) \subseteq \mathcal{I}(t_0)$ denotes the set of parked PEVs with *zero* laxity ($\theta_i(t) = 0, \forall t \in [t_0, t_0 + H)$).

Proof: The proof is intuitive. Constraint (24a) ensures the feasibility of the aggregated energy charging profile $\boldsymbol{E}$. Constraint (24b) ensures that the induced charging power $P(t) = E(t+1) - E(t)$ is at least enough to support the *non-controllable* charging demand (i.e., PEVs with $\theta_i(t) = 0$) at each time t. Based on MLLLP, we know the parked PEVs with *zero* laxity is prioritized. Therefore, the feasibility of solution can be recursively ensured. ∎

We illustrate the complete framework of our approach in Fig. 4 which includes the following five steps.

Step 1: At each time t_0, collect all the available information which includes the charging requests of new arrivals, the predictions of the RES over the predicted horizon H, the stored hydrogen in the HES and the ToU price.

Step 2: Aggregate the charging demand of the parked PEVs and determine the policy space Θ for (α^e, β^e).

Step 3: Randomly sample $|S|$ policies from Θ and construct the sampled policy space Θ^e.

Step 4: Simulate the sampled policy space Θ^e and select the *observed best* by ranking their operation cost in a non-decreasing order.

Step 5: Distribute the aggregated charging policy among the parked PEV with the MLLLP principle based method.

IV. NUMERICAL RESULTS

A. Simulation Settings

We consider a CS run by a smart building with the service capacity of $N = 400$. We study the PEV charging scheduling
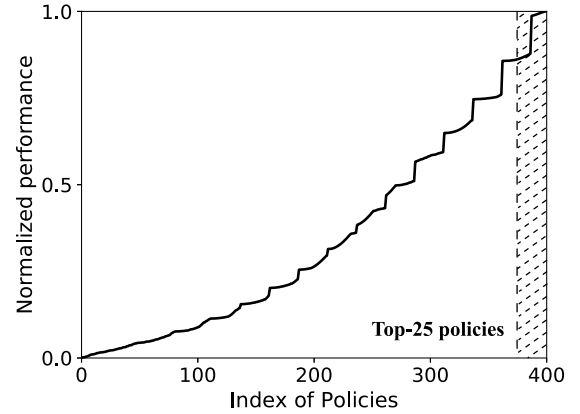

Fig. 5. The normalized **OPC** of PEV charging scheduling.

for the CS on a daily basis with the computing epoch $\Delta T = 15$ min and the prediction horizon $H = 8$ (2h). The parameter settings for the wind turbine, solar panels, HES, CS and PEV are shown in Table I. The historical meteorological data (i.e., solar radiation and wind speed profiles) [40] are used to capture the uncertain renewable generation in our simulation. Besides, we use the real traffic data of Shanghai, China [41] to simulate the charging requirements of PEVs. We refer to the TOU price in [42]. This experiment is run on a desktop with a 4 core 3.2-GHz Intel i5-4460 processor and 8 GB RAM.

B. OO Settings

For the OO implementation, we assume that the prediction error of the RES is $\delta = 10\%$ and set **AP** = 0.95, $k = 2$, $|g| = 25$ and **SR** = "blind pick" (random sampling). The interpretation is that we expect at least $k = 2$ policies over the **simulated** set S will be in **real Good Enough** set G (i.e., real top-25) with a probability of 95%. To be noted, the carnality g is totally decided by our sense of **Good Enough**. Besides, we equally discretize the ranges of α^e and β^e into 20 and we thus have a policy space $|\Theta| = 20^2 = 400$ for sampling. To identify the **OPC** class, we simulate and rank the policies in Θ by their performance, and then we can obtain the normalized **OPC** curve shown in Fig. 5. The numerical results show that the PEV charging scheduling problem has a "Flat" **OPC**. We indicate the real top-25 best policies in shadow which are the **Good Enough** polices to be obtained via OO.

TABLE II
PERFORMANCE OF THE DIFFERENT POLICIES

| Policy | Predc. | | Cost | | | Computation |
	10%	5%	Mean ($\times 10^3$CNY)	Std. ($\times 10^3$CNY)	Inc. (%)	ACT (sec.)
BM-P	✓		25.30	0.91	-	319.7
OO-P	✓		25.89	0.94	+ 2.33	0.5
OO-P(5%)		✓	24.13	0.79	- 4.62	0.4
Opt-P_C	✓		27.19	1.06	+ 7.47	0.4
CToU	-	-	33.72	1.52	+ 33.28	-

Further, we compute the required size of simulated set S for implementation: $Z(25, 2) = 131$ which means $|S| = 131$ over the policy space $|\Theta| = 400$ will be randomly simulated.

C. Performance Analysis

To evaluate the performance of the proposed method in the CS operation cost reduction and computation efficiency, we make the following comparisons.

1) BM-P: The optimal solution obtained by solving the original problem (13) with CPLEX based on the predicted information. We use this as a benchmark to quantify the performance gap.

2) OO-P: Our proposed OO-based method and use the predicted information. This supposes to be used for practice.

3) OO-P(5%): Our proposed OO-based method but assumed with prediction accuracy $\delta = 5\%$. This is designed to study the effect of noise level (i.e., prediction accuracy) on the performance of OO-based method.

4) Opt-P_C [15]: A real-time PEV charging scheduling method that first decides the aggregated charging power P_C by achieving valley-filling and then distribute it among the parked PEVs by their charging priority index defined as the proportion of remaining charging energy and the remaining charging time.

5) CToU: A heuristic rule where we first use the free renewable energy to support the PEV charging demand and then purchase the shortfall at the time-period with the lowest price over each planning horizon H.

The settings (i.e., the information used) along with the numeric results (i.e., the CS operation cost and average computing time) of different methods are shown in Table II. Particularly, though the service capacity of the CS is $N = 400$ (charging piles), it can provide PEV charging services to several times of that number as the PEVs will come and leave over the time. Therefore, the operation cost is the total charging cost for all the served PEVs over the day.

We first look into the comparisons under 10% prediction error (i.e., BM-P, OO-P, Opt-P_C and CToU). We find that BM-P provides the lowest operation cost. This is reasonable since it solves the optimization problem (13) comprehensively and supposes to provide the optimal bound. However, BM-P requires much higher computation expense (319.7 seconds) over the others (less than one second). To be noted, our OO-P has a performance gap of 2.33% but shows high computation efficiency (less than one second). When comparing our OO-P with the existing real-time scheduling method Opt-P_C, we see

they have equal high computation efficiency but our OO-P can provides lower performance degradation, i.e., 2.33% vs. 7.47%. The underlying reason is that Opt-P_c aims for valley-filling instead of operation cost reduction for the CS. Further, the comparison with CToU has demonstrated the superiority of OO-P for optimizing the operation cost over the heuristic rule. The latter usually provide an experience-based solution but leave big room for performance improvement.

Considering the uncertainties, we also studied the impact of noise level (i.e., prediction error of renewable generation) on the performance of OO-P. From the numeric results with $\delta = 5\%$ (OO-P(5%)) and $\delta = 10\%$ (OO-P) noise level, we have some insight that the performance of OO-P can be further enhanced by improving the prediction accuracy of the renewable generation over the predicted horizon H. The essential impact of noise level δ is that it will affect our observations with the simulated set S. More specifically, when there is no noise, we are sure that the **observed best** is exactly the **real best** within the simulated set S. However, if there exists noise, the **observe best** may not be the **real best** in realization due to the prediction error of the renewable generation. To further illustrate it, we have used a time instant as an example and inspected the top-10 **observed best** policy and their **real cost** under different realizations. Fig. 6 shows three cases that may happen: *i)* the **observed best** is exactly the real best within the simulated set S; *ii)* the **observe best** is not the **real best** but still shows desirable performance in realization (i.e., the **real** third-best is identified as the observed best in this case); and *iii)* the **observed best** is actually infeasible in realization.

D. Scalability Analysis

To evaluate the scalability of the proposed OO-P, we have increased the service capacity of CS to $N = 700, 1200, 2000$. The other parameter settings are the same as Section IV-A. We compare the proposed OO-P with BM-P, Opt-P_C and CToU under the noise level of $\delta = 10\%$ (i.e., prediction error of the renewable generation). For the different scales and methods, the induced operation cost and the average computing time (ACT) are shown in Table III. Overall, we can observe similar results as discussed in Section IV-C. Specifically, as a benchmark of optimal bound, BM-P provides the lowest operation cost over the other methods. However, the computation burden represents a issue for large scale practice. For example, it takes about 25 min for BM-P to obtain the optimal charging policy from solving the optimization problem (13). Moreover, we see that the ACT is superlinear w.r.t. the scale N. Therefore, it does not scale well for implementation. Importantly, the performance gap of our OO-P over BM-P is no more than 4% with all the scales. However, OO-P shows much higher computation efficiency (i.e., at second level). Moreover, we only see a minor increase of ACT w.r.t. the scale N. The underlying reason is that we have scale down the decision variables to $O(2)$ by proposing a parameterized aggregated model, and thus make OO-P almost not restricted to the scale. Besides, compared with the existing real-time PEV scheduling method Opt-P_c, OO-P shows less performance discount over the optimal (BM-P), showing about 6% more operation cost
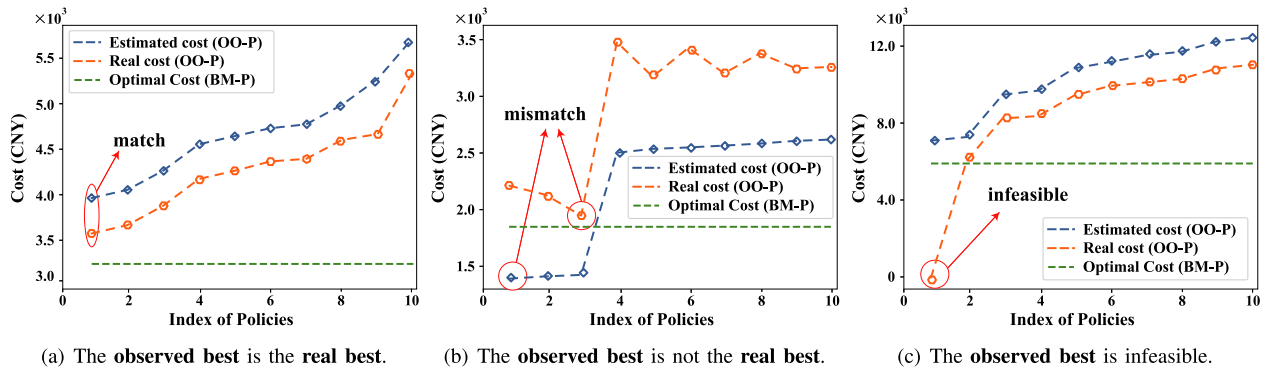
(a) The **observed best** is the **real best**. (b) The **observed best** is not the **real best**. (c) The **observed best** is infeasible.

Fig. 6. Three cases of observations with the simulated set S.

TABLE III
THE PERFORMANCE FOR LARGE SCALES WITH THE DIFFERENT METHODS

| Policy | $N = 700$ | | | $N = 1200$ | | | $N = 2000$ | | |
	Cost ($\times 10^4$CNY)	Inc. (%)	ACT (sec.)	Cost ($\times 10^4$CNY)	Inc. (%)	ACT (sec.)	Cost ($\times 10^4$CNY)	Inc. (%)	ACT (sec.)
BM-P	4.60	-	575.68	8.03	-	1532.61	12.91	-	3712.41
OO-P	4.75	+ 3.26	0.97	8.31	+ 3.49	1.77	13.41	+ 3.87	3.38
Opt-P_C	5.05	+ 9.78	0.58	8.83	+ 9.96	0.84	13.95	+ 8.06	1.49
CToU	6.27	+ 36.30	-	10.93	+ 36.11	-	17.57	+ 36.10	-

TABLE IV
PERFORMANCE OF OO-P WITH DIFFERENT (k, g) SETTINGS

| Para. | | | Performance | | Para. | | | Performance | |
k	g	s	Cost ($\times 10^2$CNY)	ACT (sec.)	k	g	s	Cost ($\times 10^2$CNY)	ACT (sec.)
2	10	403	80.17	0.79	6	10	1070	73.13	1.72
2	20	179	73.69	0.51	6	20	468	73.14	0.88
2	30	112	77.09	0.42	6	30	289	78.12	0.64
2	40	81	79.90	0.38	6	40	206	77.89	0.53
4	10	746	78.06	1.24	8	10	1383	78.79	2.07
4	20	327	71.96	0.69	8	20	603	76.20	1.05
4	30	203	81.32	0.52	8	30	373	72.97	0.73
4	40	145	77.16	0.46	8	40	265	75.91	0.60

reduction for the CS. Obviously, we see OO-P outperforms the heuristic rule CToU in optimizing the operation cost with all the scales.

E. OO Parameter Analysis

As aforementioned, the settings of OO-P (i.e., the **Alignment Level** k and the carnality of **Good Enough** set g) will affect the performance (i.e., the CS operation cost). To give some insights, we use the case with a CS service capacity $N = 100$ as an example to study the performance of OO-P with the different settings of (k, g). We first decide the required size of simulated set S according to (22) and then perform OO-P for the different settings. The induced operation cost and the average computing time (ACT) are shown in Table IV.

First, we can spot that a larger **Alignment Level** k plus a smaller **Good Enough** set g will induce a larger **simulated** set s to be simulated and evaluated. For example, when we

set $k = 8$ and $g = 10$, we will require a **simulated** set of size $s = 1383$. That will slightly increase the computing time.

Besides, when the **Alignment Level** k is fixed, we observe the performance of OO-P first increases and then begins to drop w.r.t. the carnality of **Good Enough** set s. For example, when we set $k = 2$ (the top-left block), we see the operation cost decrease when we increase from $g = 10$ to $g = 20$. However, when we keep increasing to $g = 30$ and $g = 40$, the performance drops. This implies for some fixed **Alignment Level** k, there exists an appropriate carnality of **Good Enough** set g to achieve better performance.

We can observe the same trend when we fix g and increase k. These results show that in the real-time operation, the CS needs to choose the appropriate parameter settings for OO-P to achieve a better economic benefits.

V. CONCLUSION

In this paper, we studied the real-time operation of a public charging station (CS) providing charging service to large-scale PEVs. To enable a computationally efficient and scalable implementation, we first developed a parameterized aggregated PEV charging model based on the problem structure, which can largely scale down the decision variables from $O(NH)$ to $O(2)$. This makes it possible to apply the ordinal optimization (OO) technique to search for good enough parameterized aggregated charging policy within the 2D decision space. After that, we modify the existing Less Laxity and Longer Remaining Processing Time (LLLP) principle [27] to distribute the aggregated charging profile among the individual PEVs. We demonstrated that the proposed method can ensure high computation efficiency and scalability at the expense of a minor performance degradation (i.e., no more than 4%). Our method also outperforms the existing real-time and heuristic

PEV charging scheduling methods in reducing the operation cost for the CS. This paper can work as an example that how the soft optimization technique and problem structure can be explored to achieve the performance improvement of complex dynamic systems.

REFERENCES

[1] *The Global Electric Vehicle Market in 2021: Statistics & Forecasts*. Accessed: Feb. 12, 2021. [Online]. Available: https://www.virta.global/global-electric-vehicle-market?__hstc=51530422.4f85461c5a4a172642cb54421d73da8b.1612998885893.1612998885893.1612998885893.1&__hssc=51530422.1.1612998885894&__hsfp=3869317212&hsutk=4f85461c5a4a172642cb54421d73da8b&contentType=standard-page#nine

[2] A. Ipakchi and F. Albuyeh, "Grid of the future," *IEEE Power Energy Mag.*, vol. 7, no. 2, pp. 52–62, Mar./Apr. 2009.

[3] M. Muratori, "Impact of uncoordinated plug-in electric vehicle charging on residential power demand," *Nat. Energy*, vol. 3, no. 3, pp. 193–201, 2018.

[4] K. Jhala, B. Natarajan, A. Pahwa, and L. Erickson, "Coordinated electric vehicle charging for commercial parking lot with renewable energy sources," *Elect. Power Compon. Syst.*, vol. 45, no. 3, pp. 344–353, 2017.

[5] M. Longo, "A electric vehicles integrated with renewable energy sources for sustainable mobility," in *New Trends in Electrical Vehicle Powertrains*. London, U.K.: IntechOpen, 2019, pp. 203–223.

[6] A. S. Al-Ogaili *et al.*, "Review on scheduling, clustering, and forecasting strategies for controlling electric vehicle charging: Challenges and recommendations," *IEEE Access*, vol. 7, pp. 128353–128371, 2019.

[7] Z. Yang, K. Li, and A. Foley, "Computational scheduling methods for integrating plug-in electric vehicles with power systems: A review," *Renew. Sustain. Energy Rev.*, vol. 51, pp. 396–416, Nov. 2015.

[8] J. C. Mukherjee and A. Gupta, "A review of charge scheduling of electric vehicles in smart grid," *IEEE Syst. J.*, vol. 9, no. 4, pp. 1541–1553, Dec. 2015.

[9] Y. Yang, Q.-S. Jia, X. Guan, X. Zhang, Z. Qiu, and G. Deconinck, "Decentralized EV-based charging optimization with building integrated wind energy," *IEEE Trans. Autom. Sci. Eng.*, vol. 16, no. 3, pp. 1002–1017, Jul. 2019.

[10] Z. Ma, D. S. Callaway, and I. A. Hiskens, "Decentralized charging control of large populations of plug-in electric vehicles," *IEEE Trans. Control Syst. Technol.*, vol. 21, no. 1, pp. 67–78, Jan. 2013.

[11] S. Bahrami and M. Parniani, "Game theoretic based charging strategy for plug-in hybrid electric vehicles," *IEEE Trans. Smart Grid*, vol. 5, no. 5, pp. 2368–2375, Sep. 2014.

[12] M. Hong, S. Zeng, J. Zhang, and H. Sun, "On the divergence of decentralized non-convex optimization," 2020. [Online]. Available: arXiv:2006.11662.

[13] Q.-S. Jia and J. Wu, "A structural property of charging scheduling policy for shared electric vehicles with wind power generation," *IEEE Trans. Control Syst. Technol.*, early access, Dec. 9, 2020, doi: 10.1109/TCST.2020.3040572.

[14] T. Wu, Q. Yang, Z. Bao, and W. Yan, "Coordinated energy dispatching in microgrid with wind power generation and plug-in electric vehicles," *IEEE Trans. Smart Grid*, vol. 4, no. 3, pp. 1453–1463, Sep. 2013.

[15] Y. Zheng, Y. Shang, Z. Shao, and L. Jian, "A novel real-time scheduling strategy with near-linear complexity for integrating large-scale electric vehicles into smart grid," *Appl. Energy*, vol. 217, pp. 1–13, May 2018.

[16] E. Bagherzadeh, A. Ghiasian, and A. Rabiee, "Long-term profit for electric vehicle charging stations: A stochastic optimization approach," *Sustain. Energy Grids Netw.*, vol. 24, Dec. 2020, Art. no. 100391.

[17] O. Fallah-Mehrjardi, M. H. Yaghmaee, and A. Leon-Garcia, "Charge scheduling of electric vehicles in smart parking-lot under future demands uncertainty," *IEEE Trans. Smart Grid*, vol. 11, no. 6, pp. 4949–4959, Nov. 2020.

[18] P. Kou, D. Liang, L. Gao, and F. Gao, "Stochastic coordination of plug-in electric vehicles and wind turbines in microgrid: A model predictive control approach," *IEEE Trans. Smart Grid*, vol. 7, no. 3, pp. 1537–1551, May 2016.

[19] Y. Guo, J. Xiong, S. Xu, and W. Su, "Two-stage economic operation of microgrid-like electric vehicle parking deck," *IEEE Trans. Smart Grid*, vol. 7, no. 3, pp. 1703–1712, May 2016.

[20] Y. Yang, Q.-S. Jia, and X. Guan, "Stochastic coordination of aggregated electric vehicle charging with on-site wind power at multiple buildings," in *Proc. IEEE 56th Annu. Conf. Decis. Control (CDC)*, 2017, pp. 4434–4439.

[21] Y. Yang, Q.-S. Jia, G. Deconinck, X. Guan, Z. Qiu, and Z. Hu, "Distributed coordination of EV charging with renewable energy in a microgrid of buildings," *IEEE Trans. Smart Grid*, vol. 9, no. 6, pp. 6253–6264, Nov. 2018.

[22] Q. Huang, Q.-S. Jia, Z. Qiu, X. Guan, and G. Deconinck, "Matching EV charging load with uncertain wind: A simulation-based policy improvement approach," *IEEE Trans. Smart Grid*, vol. 6, no. 3, pp. 1425–1433, May 2016.

[23] T. Long, X.-T. Ma, and Q.-S. Jia, "Bi-level proximal policy optimization for stochastic coordination of EV charging load with uncertain wind power," in *Proc. IEEE Conf. Control Technol. Appl. (CCTA)*, 2019, pp. 302–307.

[24] K. L. López, C. Gagné, and M.-A. Gardner, "Demand-side management using deep learning for smart charging of electric vehicles," *IEEE Trans. Smart Grid*, vol. 10, no. 3, pp. 2683–2691, May 2019.

[25] T. Ding, Z. Zeng, J. Bai, B. Qin, Y. Yang, and M. Shahidehpour, "Optimal electric vehicle charging strategy with Markov decision process and reinforcement learning technique," *IEEE Trans. Ind. Appl.*, vol. 56, no. 5, pp. 5811–5823, Sep./Oct. 2020.

[26] S. Wang, S. Bi, and Y. A. Zhang, "Reinforcement learning for real-time pricing and scheduling control in EV charging stations," *IEEE Trans. Ind. Informat.*, vol. 17, no. 2, pp. 849–859, Feb. 2021.

[27] Y. Xu, F. Pan, and L. Tong, "Dynamic scheduling for charging electric vehicles: A priority rule," *IEEE Trans. Autom. Control*, vol. 61, no. 12, pp. 4094–4099, Dec. 2016.

[28] M. A. Mirzaei, A. S. Yazdankhah, and B. Mohammadi-Ivatloo, "Stochastic security-constrained operation of wind and hydrogen energy storage systems integrated with price-based demand response," *Int. J. Hydrogen Energy*, vol. 44, no. 27, pp. 14217–14227, 2019.

[29] K. Grogg, "Harvesting the wind: The physics of wind turbines," *Phys. Astron. Comps Papers*, vol. 7, pp. 1–42, 2005.

[30] L. Pengfei, "Study on capacity optimal configuration and energy management of integrated wind-solar-hydrogen-storage power supply system," Ph.D. dissertation, Dept. Comput. Sci., Zhejaing Univ., Hangzhou, China, 2017.

[31] Z. Jimin, "Performance simulation and energy management of hybrid wind-pemfc power generation system," Ph.D. dissertation, Dept. Elect. Eng., Shandong Univ., Jinan, China, 2017.

[32] M. E. Kabir, C. Assi, M. H. K. Tushar, and J. Yan, "Optimal scheduling of EV charging at a solar power-based charging station," *IEEE Syst. J.*, vol. 14, no. 3, pp. 4221–4231, Sep. 2020.

[33] H. Zhang, Z. Hu, Z. Xu, and Y. Song, "Evaluation of achievable vehicle-to-grid capacity using aggregate PEV model," *IEEE Trans. Power Syst.*, vol. 32, no. 1, pp. 784–794, Jan. 2017.

[34] Y.-C. Ho, R. Sreenivas, and P. Vakili, "Ordinal optimization of DEDs," *Discr. Event Dyn. Syst.*, vol. 2, no. 1, pp. 61–88, 1992.

[35] S. Nanchian, A. Majumdar, and B. C. Pal, "Ordinal optimization technique for three-phase distribution network state estimation including discrete variables," *IEEE Trans. Sustain. Energy*, vol. 8, no. 4, pp. 1528–1535, Oct. 2017.

[36] T. Ma, F. Tian, and B. Dong, "Ordinal optimization-based performance model estimation method for HDFs," *IEEE Access*, vol. 8, pp. 889–899, 2019.

[37] S.-C. Horng and S.-S. Lin, "Ordinal optimization based metaheuristic algorithm for optimal inventory policy of assemble-to-order systems," *Appl. Math. Model.*, vol. 42, pp. 43–57, Feb. 2017.

[38] J. Dutka, "The incomplete beta function—A historical profile," *Archive History Exact Sci.*, vol. 24, no. 1, pp. 11–29, 1981.

[39] Y.-C. Ho, Q.-C. Zhao, and Q.-S. Jia, *Ordinal Optimization: Soft Optimization for Hard Problems*. New York, NY, USA: Springer, 2008.

[40] *The National Meteorological Information Center*. Accessed: May 10, 2021. [Online]. Available: http://data.cma.cn/en

[41] *Taxis—Smart City Research Group*. Accessed: May 10, 2021. [Online]. Available: https://www.cse.ust.hk/scrg/

[42] T. Long and Q.-S. Jia, "Matching uncertain renewable supply with EV charging demand—A bi-level event-based optimization method," *Complex Syst. Model. Simulat.*, to be published.